JACS
JOURNAL OF THE AMERICAN CHEMICAL SOCIETY
Article
pubs.acs.org/JACS

# Enzyme Substrate Specificity Conferred by Distinct Conformational Pathways

Florencia Rago,[†,⊥] Daniel Saltzberg,[‡,∥] Karen N. Allen,[*,§,†] and Dean R. Tolan[*,†,¶]

[†]Program in Biochemistry and Molecular Biology (BMB), Boston University, Boston, Massachusetts 02215, United States
[‡]Department of Physiology and Biophysics, Boston University School of Medicine, Boston, Massachusetts 02118, United States,
[§]Department of Chemistry, Boston University, Boston, Massachusetts 02215, United States,
[¶]Department of Biology, Boston University, Boston, Massachusetts 02215, United States

Supporting Information

**ABSTRACT:** Substrate recognition is one of the hallmarks of enzyme catalysis. Enzyme conformational changes have been linked to selectivity between substrates with little direct evidence. Aldolase, a glycolytic enzyme, must distinguish between two physiologically important substrates, fructose 1-phosphate and fructose 1,6-bisphosphate, and provides an excellent model system for the study of this question. Previous work has shown that isozyme specific residues (ISRs) distant from the active site are responsible for kinetic distinction between these substrates. Notably, most of the ISRs reside in a cluster of five surface α-helices, and the carboxyl-terminal region (CTR), and cooperative interactions among these helices have been demonstrated. To test the hypothesis that conformational changes are at the root of these changes, single surface-cysteine variants were created with the cysteine located on helices of the cluster and CTR. This allowed for site-specific labeling with an environmentally sensitive fluorophore, and subsequent monitoring of conformational changes by fluorescence emission spectrophotometry. These labeled variants revealed different spectra in the presence of saturating amounts of each substrate, which suggested the occurrence of different conformations. Emission spectra collected at various substrate concentrations showed a concentration dependence of the fluorescence spectra, consistent with binding events. Lastly, stopped-flow fluorescence spectrophotometry showed that the rate of these fluorescence changes was on the same time-scale as catalysis, thus suggesting a link between the different fluorescence changes and events during catalysis. On the basis of these results, we propose that different conformational changes may be a common mechanism for dictating substrate specificity in other enzymes with multiple substrates.

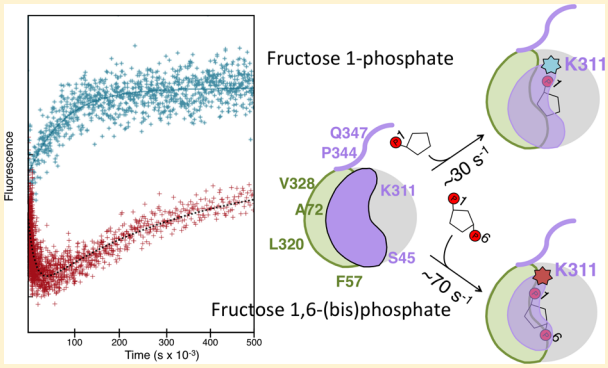


## INTRODUCTION

Since the concept of induced fit was first proposed, biochemists have considered protein conformational changes important for catalysis.[1,2] Although the effects of induced fit have historically focused on the conformation at the active site, it is becoming increasingly evident that conformational changes occurring in regions distant from the active site also play an important role in catalysis and in dictating substrate specificity.[2−5] Studies using a combination of fluorescence, computer modeling, mutagenesis, NMR, and crystallography have shown the importance of such conformational changes in the function of a number of enzymes. For example, in the case of dihydrofolate reductase (DHFR), backbone and side-chain motions are essential for cofactor binding, substrate binding, and catalysis.[5,6] Thus, the innate mobility of the protein scaffold allows the dynamics that are critical in the various steps of the catalytic cycle. Indeed, extensive studies of hydrogen transfer in proteins are consistent with the concept that protein dynamics create transient conformations with a favorable electrostatic environment for proton and hydride transfer.[4,7] In the case of proline isomerase, the enzyme adopts alternate conformations and the rate of switching between these conformations correlates with changes in rates of catalysis.[8] However, how such dynamics affect substrate specificity has never been elucidated. In particular, how different rates of turnover for different substrates are achieved via different conformational pathways has never been demonstrated.

Like many enzymes that must distinguish among various substrates, the glycolytic enzyme aldolase can cleave either fructose 1,6-bisphosphate (Fru 1,6-$P_2$) during glycolysis or fructose 1-phosphate (Fru 1-P) during fructose metabolism. The differing importance of these two processes in diverse tissues is likely one root of the evolutionary pressure for the divergence of three different isozymes in mammals, aldolases A, B, and C. These three isozymes show differences in specificity

**Received:** August 3, 2015
**Published:** October 6, 2015



DOI: 10.1021/jacs.5b08149
J. Am. Chem. Soc. 2015, 137, 13876−13886

**Scheme 1. The Uni-bi Aldolase Mechanism**[a]

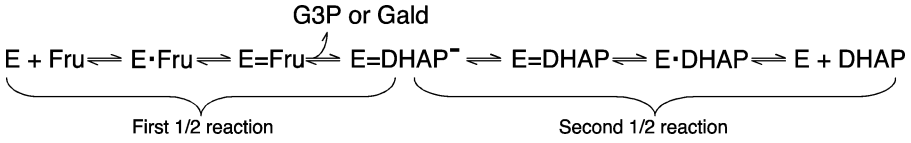


[a]Fru is either Fru 1,6-$P_2$ or Fru 1-P. Non-covalent (•) or covalent (=) bonds to E are indicated. G3P is glyceraldehyde 3-phosphate, Gald is glyceraldehyde, DHAP is dihyroxyacetone phosphate.

toward these two hexoses that reflect their physiological roles in the tissues in which they are expressed.[9] The uni-bi aldolase-catalyzed cleavage reaction can be divided into two half-reactions[10] (Scheme 1). The first half-reaction involves hexose binding, ring-opening,[11] C−C bond cleavage using covalent catalysis via a Schiff base, and release of the first product, an aldotriose. The second half-reaction involves enamine protonation, hydrolysis of the Schiff base, and release of the second ketotriose, dihydroxyacetone phosphate (DHAP). Notably, the second half-reaction is chemically identical for both hexose substrates, and the last step, DHAP release, is rate limiting for Fru 1,6-$P_2$ cleavage.[12,13] For Fru 1-P cleavage, this second half reaction is likely the rate-limiting step as well,[14] yet the rates of cleavage (reflected in $k_{cat}$ values) of these two hexoses can differ by 10−20 fold.[9] This results in an interesting conundrum: how do identical second half reactions operate at different rates? Herein, a model that conformational changes account for the differences in the $k_{cat}$ values for the different substrates, realized in the second half-reaction but initiated by binding in the first half-reaction, is tested.

Insights into this paradox and the role that conformational changes may play have been considered previously for aldolases.[15,16] In particular, oxidation of two nonadjacent Cys residues (>10 Å apart) curtails aldolase A activity, and the two substrates protect against this inactivation to different extents.[16,17] Support for the connection between cysteine oxidation and activity loss comes from analysis of an engineered variant of aldolase A without any surface Cys residues, which is resistant to oxidative inactivation.[18]

Despite the differences in specificity, the crystal structures for all three isozymes show superimposable active sites[19,20] and there is no observable difference in conformation in the presence and absence of substrates, except for the structure of the CTR.[21,22] Further understanding was gained from studies of the evolutionarily conserved isozyme-specific residues (ISRs), which are necessary and sufficient for isozyme-specific kinetic behavior.[23] Aldolase ISRs are far from the active site, largely on the surface, and cluster into two patches (a distal surface patch (DSP) and a terminal surface patch (TSP)), which map to a previously unappreciated cluster comprising a five $\alpha$-helical bundle ($\alpha$2, $\alpha$3, $\alpha$4, $\alpha$13, and $\alpha$14) plus the CTR. The closest ISR residues are >8 Å from any active-site residue. While not interacting directly with the active site, the ISRs in the TSP and DSP appear to be codependent in defining $k_{cat}/K_m$ values for each substrate.[17] Could these patches be involved in differential conformational changes that participate in defining substrate specificity?

Herein a refinement of the model proposed above is tested; specifically, does the substrate-dependent conformational flexibility of the $\alpha$-helical cluster explain the kinetic differences between substrates? In addition, the rates of conformational changes of elements within the patches may reveal a mechanism for how these enzyme dynamics are involved in the aldolase catalytic cycle. Nonconserved residues in the $\alpha$-helical bundle in the DSP and TSP were empirically chosen for modification to report on environmental changes when adducted with a conformation-sensitive fluorescent probe. The fluorescently labeled proteins were subsequently studied using ensemble methods for changes in fluorescence in the presence or absence of each hexose; Fru 1,6-$P_2$ or Fru 1-P. The magnitude of fluorescence changes was different with each hexose, suggesting a mechanism by which aldolase substrate specificity is conferred by these differential conformational changes. Dependence of the fluorescence changes on substrate concentration indicated that binding events are linked to the conformational changes. The rates of these dynamic transitions were measured by stopped-flow fluorescence and the data showed these dynamics were within the time scale of the catalytic cycle and differ markedly between substrates. Together, the detected fluorescence differences were correlated to conformational changes that differed depending on the substrate used, and had rates of change that could explain the conundrum of the aldolase half reactions discussed above. This work suggests that aldolase may distinguish between substrates by differing substrate-triggered conformational changes.

## EXPERIMENTAL SECTION

**Site-Directed Mutagenesis and Variant Construction.** Specific nucleotide changes were made in rabbit aldolase A cDNA sequences via site-directed mutagenesis as previously described.[23,24] Cysteine mutations were made at residues S45, F57, A72, S131, K311, V320, L328, Q347, and P344 on a "cys-lite"-aldolase A variant (gTet) that has all four surface Cys substituted by Ala in the expression plasmid pPB1.[17,25]

**Protein Expression and Purification.** Variant aldolases were expressed in *Escherichia coli* and purified at 4 °C as described previously.[26] Briefly, cells expressing the variant aldolases were pelleted and washed with a 0.15 M NaCl solution. The cells were resuspended in 250 mM MOPS, pH 7.0, 10 mM EDTA, 2 mM DTT, 1% (v/v) glycerol, 0.1 $\mu$g/mL pepstatin A, 0.1 mg/mL DNase I, 0.1 mg/mL RNase A, and 2.5 mM PMSF and lysed using a French Press at 20 000 psi. Two rounds of centrifugation at 37 000*g* and 50 000*g* cleared the lysate. The soluble fraction was subsequently treated with 70% saturated ammonium sulfate, the resulting pellet was resuspended in MGK buffer (50 mM MOPS-glycine-KOH, pH 7.0 (except at pH 6.5 for purification of variant K311C), and 0.1 mM DTT), and the solution dialyzed overnight in MGK. The dialyzed sample was bound to CM Sepharose Fast Flow resin, washed with MGK buffer, and eluted using 2.5 mM Fru 1,6-$P_2$ in MGK. Fractions were pooled and brought to 70% saturation in ammonium sulfate and 2 mM DTT and stored at 4 °C. Before use proteins were dialyzed against 100 mM Tris-HCl, pH 8.4, and 0.1 mM DTT.

**Assay for Aldolase Activity.** Aldolase activity for hexose cleavage was measured at 30 °C using a coupled assay that monitors the rate of NADH oxidation at 340 nm.[26,27] Aldolase was added to the reaction mixture (50 mM triethanolamine, pH 7.4, 10 mM Na-EDTA, 0.001% (v/v) glycerol-3-phosphate dehydrogenase/triosephosphate isomerase, 0.15 mM NADH) at 0.8 $\mu$g/mL for Fru 1,6-$P_2$ assays and 15 $\mu$g/mL for Fru 1-P assays. Substrate concentration was varied between 1 and


DOI: 10.1021/jacs.5b08149
J. Am. Chem. Soc. 2015, 137, 13876−13886

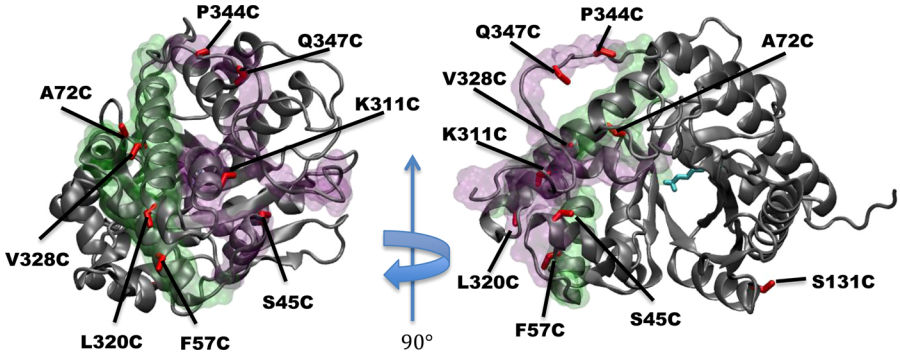


**Figure 1.** Sites of MDCC-labeling on the aldolase monomer. A single monomer (PDB: 1ADO, subunit A) is depicted in two orientations rotated by 90° on the *y*-axis. Sites on the aldolase monomer that were chosen for individual site-directed mutagenesis to create a cysteine substitution for subsequent attachment of a fluorescent probe are shown in red sticks. The TSP is shown in transparent purple surface rendering of $\alpha$-helices 2, 13, and the CTR. The DSP is shown in transparent green surface rendering of $\alpha$-helices 3, 4, and 14. The active site is marked by a cyan stick depiction of K229, including the polar hydrogens. Figure created using VMD.[30]

1200 $\mu$M for Fru 1,6-$P_2$ and 1 and 10 mM for Fru 1-P. Protein concentration was determined as described by Bradford.[28]

**Assay for Thiol Groups.** Dithiothreitol was removed from samples by gel filtration using BioGel P6DG and diluted to 1 mg/mL in 100 mM Tris-HCl, pH 8.4. Protein (0.1 mL) was added to a 96-well plate containing 0.1 mL of 3 mM DTNB in 100 mM Tris-HCl, pH 9.4. The reaction was allowed to incubate for 5 min at 25 °C and absorbance at 412 nm was recorded. To quantify both buried and surface thiol groups, the protein solution was first incubated with 1% (w/v) SDS for 15 min and then treated as above. The number of sulfhydryls present on the proteins was determined using $\varepsilon$ = 13 600 $M^{-1}$ $cm^{-1}$.

**Fluorescent Labeling.** Labeling reactions were carried out in GET buffer (50 mM TEA-HCl, pH 8.0, 20% (v/v) glycerol, 2 mM EDTA). Proteins were labeled with MDCC by either of two methods with no significant differences in labeling efficiency or product quality observed. Proteins were first dialyzed against GET containing 0.5 mM DTT for 6 h, then with no DTT for 2 h, and any remaining DTT was subsequently removed by gel filtration using BioGel P6DG. The protein was then diluted to 50 $\mu$M in 1 mL of GET buffer. MDCC was added dropwise while constantly stirring over 5 min to a concentration of 0.25 mM and incubated in the dark at 25 °C while stirring. After 14 h, the reaction was quenched with 5 mM DTT and excess fluorophore was removed by gel filtration using BioGel P6DG. Otherwise, proteins were labeled using a protocol adapted from Kim et al. (2008).[29] Briefly, 2 mg of aldolase in 70% ammonium-sulfate slurry was incubated for 2 h or overnight in 5 mM DTT. The protein was then centrifuged at 13 000*g* for 10 min at 4 °C. The pellet was washed three times using ice-cold GET buffer with 70% $(NH_4)_2SO_4$ (GETAS buffer). The pellet was resuspended in 1 mL of GETAS containing 500 $\mu$M MDCC and allowed to incubate for 2 h at room temperature while stirring. The reaction was quenched with 5 mM DTT and the excess fluorophore removed by gel filtration using Toyopearl HW-40F equilibrated with GET. Proteins used for bulk fluorescence measurements in the fluorimeter were resuspended in a final solution containing glycerol (a component of GET), whereas the samples used in the stopped flow experiments were resuspended in a final solution containing no glycerol (ET buffer) to avoid artifact signals due to incomplete mixing as a result of the viscosity of the solutions. Substrates were dissolved in the corresponding buffers. The incorporated label was calculated using $\varepsilon_{419}$ of 5 × $10^4$ $M^{-1}$ $cm^{-1}$ and the percent incorporation was calculated from the moles of protein present.

**Fluorescence Spectra.** Spectra were taken by exciting at 419 nm in a FluoroMax 3 fluorescence spectrophotometer using 1 cm quartz cuvettes with 3 mm slit width. The emission spectra were collected from 430 to 530 nm with 4 mm slit width in 0.5 nm increments with 0.1−0.5 s integration time and data was collected using DataMax software. Each assay used 40 $\mu$g of enzyme (0.5 $\mu$M), diluted in 2 mL in the GET buffer described above. Alternatively, a 3 mm glass cuvette was used with 2 $\mu$g of protein in a final volume of 200 $\mu$L (0.25 $\mu$M). All spectra were averaged over six recordings and repeated 2−6 times. At 4 °C, starting from a Fru 1,6-$P_2$ concentration of 0.5 mM, the equilibrium concentration of Fru 1,6-$P_2$ will be 0.495 mM. The equilibrium lies far toward the hexose ($K_{eq}$ = 1 × $10^{-4}$ M). Thus, only 5 $\mu$M trioses are present at equilibrium, and most of the starting substrate remains a hexose. Furthermore, with 40 $\mu$g of enzyme (0.5 $\mu$M), and a turnover number of ∼5 $s^{-1}$ (see Table S3), the rate would be 2.5 $\mu$M/s; thus, equilibrium was reached in 2 s. Lastly, the variants in both the TSP (K311C, S45C), DSP (F57C, A72C, L320C, and V328C), and the S131C control were tested for fluorescence changes either in intensity or $\lambda_{max}$ in the presence of products, DHAP, G3P, or glyceraldehyde (1−50 mM). In all cases, no significant changes were observed. Thus, the observed changes in the presence of hexose substrates are not due to the effect of product.

**Stopped-Flow Data Collection and Analysis.** Stopped-flow data was collected on a Hi-Tech KinetAsyst Stopped-Flow System or an Applied Photophysics DX.17MV instrument equipped with the Pro-Data upgrade. Either instrument had a dead time <2 ms. For example, the DX.17MV has a dead time of 0.85−1.37 ms depending on the light guide, with a time resolution of 1−10 measurements/ms. Protein was injected at a final concentration of 3 $\mu$g in 150 $\mu$L against 150 $\mu$L of ET buffer or substrate at 4 °C (final enzyme concentration of 0.25 $\mu$M). Excitation wavelength was 419 nm, and a 455 nm filter was used for emission collection. Calibration to set the zero-time values were performed with enzyme alone and adjusted to 100 or 200 artificial fluorescence units (AFU). The data of observed fluorescence, $I(t)$, at time $t$, is assumed to be a linear combination of the response from each conformational state ($R_X$) of the protein, multiplied by its relative concentration, X($t$):

$$I(t) = R_A \cdot A(t) + R_B \cdot B(t) + R_C \cdot C(t)$$

Time course data was analyzed by fitting to multiple kinetic models. Because of the clear biphasic behavior of the K311C toward Fru-1,6-$P_2$ data, implicating three distinct fluorescent states, both two and three-state mechanisms were considered: (1) nonreversible two-state, (2) reversible two-state, (3) a nonreversible three-state, (4) three-state with a rapid equilibrium first step followed by an irreversible second step, and 5) an irreversible heterogeneous model (Figure S2A). Each time course was fit to each model using the program DynaFit (BioKin Ltd.), assuming 100% of species A at time zero, and setting the fluorescent response of species A ($R_A$) to the average fluorescence obtained from the fluorescent mutant without ligand. All other response values and kinetic constants were fit to the data using a Levendsen−Marquardt minimization algorithm in DynaFit. The best fit scheme was determined by smallest $\chi^2$ value and observation of residual plots, while overdetermined results were discarded. The fits are shown in Figure S2B.


DOI: 10.1021/jacs.5b08149
J. Am. Chem. Soc. 2015, 137, 13876−13886

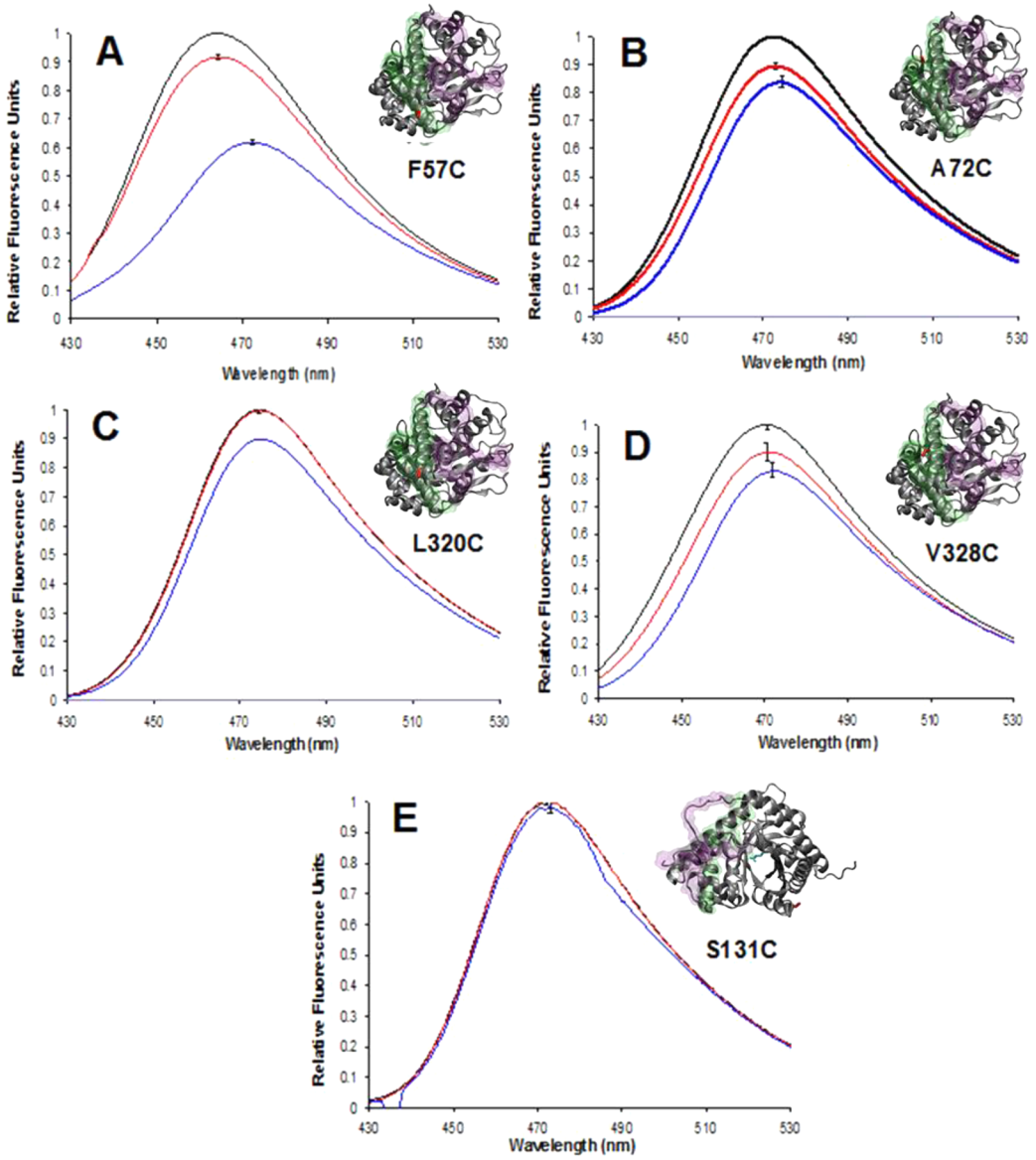


**Figure 2.** Fluorescence emission spectra of MDCC-labeled variants in the DSP and S131C. The emission spectra of the fluorescently labeled proteins are shown for the conditions: no substrate (black), Fru 1,6-$P_2$ (blue), and Fru 1-P (red). (A) F57C, (B) A72C, (C) L320C, (D) V328C, and (E) S131C. Insets showing the corresponding site of substitution are depicted as in Figure 1. Substrates were used at concentrations of 0.5 mM for Fru 1,6-$P_2$ and 10 mM for Fru 1-P. Enzyme concentration was (0.5 $\mu$M). Spectra were normalized to the maximum emission signal of the no substrate condition for each variant to give relative fluorescence units. Errors noted by bars at the emission maxima are given as 1 SD.

## RESULTS

**Substrate-Dependent Fluorescence Changes Indicate Conformational Flexibility of ISR Patches.** The mechanism by which the two patches of ISRs cooperate to confer substrate specificity could be explained by different conformational changes after substrate binding, depending on which substrate is encountered. From previous research, we identified the TSP and DSP as regions of interest[17] and identified residues that could be used to probe possible conformation changes. The TSP (Figure 1, purple) and DSP (Figure 1, green) are >9 Å apart at their closest point in all X-ray-crystal structures. The occurrence of conformational changes was probed by attachment of the fluorophore 7-diethylamino-3-[*N*-(2-maleimidoethyl) carbamoyl]coumarin (MDCC), which could report on changes of environment with and without substrate present, to several single surface-cysteine variants of a rabbit aldolase A Cys-lite[18] (F57C, A72C, L320C, and V328C in the DSP S45C, K311C, P344C, and Q347C in the TSP, and S131C outside of either). The selection of residues for Cys substitution was based on (1) their location in one of the five $\alpha$-helices or the CTR, (2) their lack of conservation among vertebrate aldolases, and (3) their partial solvent accessibility to allow fluorophore incorporation, yet also allow a conformation-dependent change in fluorescence. One site that did not match the first criteria was used as a negative control (S131C). The locations of the chosen sites are shown as a composite in Figure 1.

Each variant was constructed by site-directed mutagenesis, expressed in *Escherichia coli*, and purified as described previously.[26] Confirmation of the Cys content and assessment of the solvent accessibility was performed by reactions of DTNB with native and denatured variants (Table S1, see Supporting Information). Furthermore, each purified variant retained, within a factor of 2, wild-type substrate specificity


DOI: 10.1021/jacs.5b08149
J. Am. Chem. Soc. 2015, 137, 13876−13886

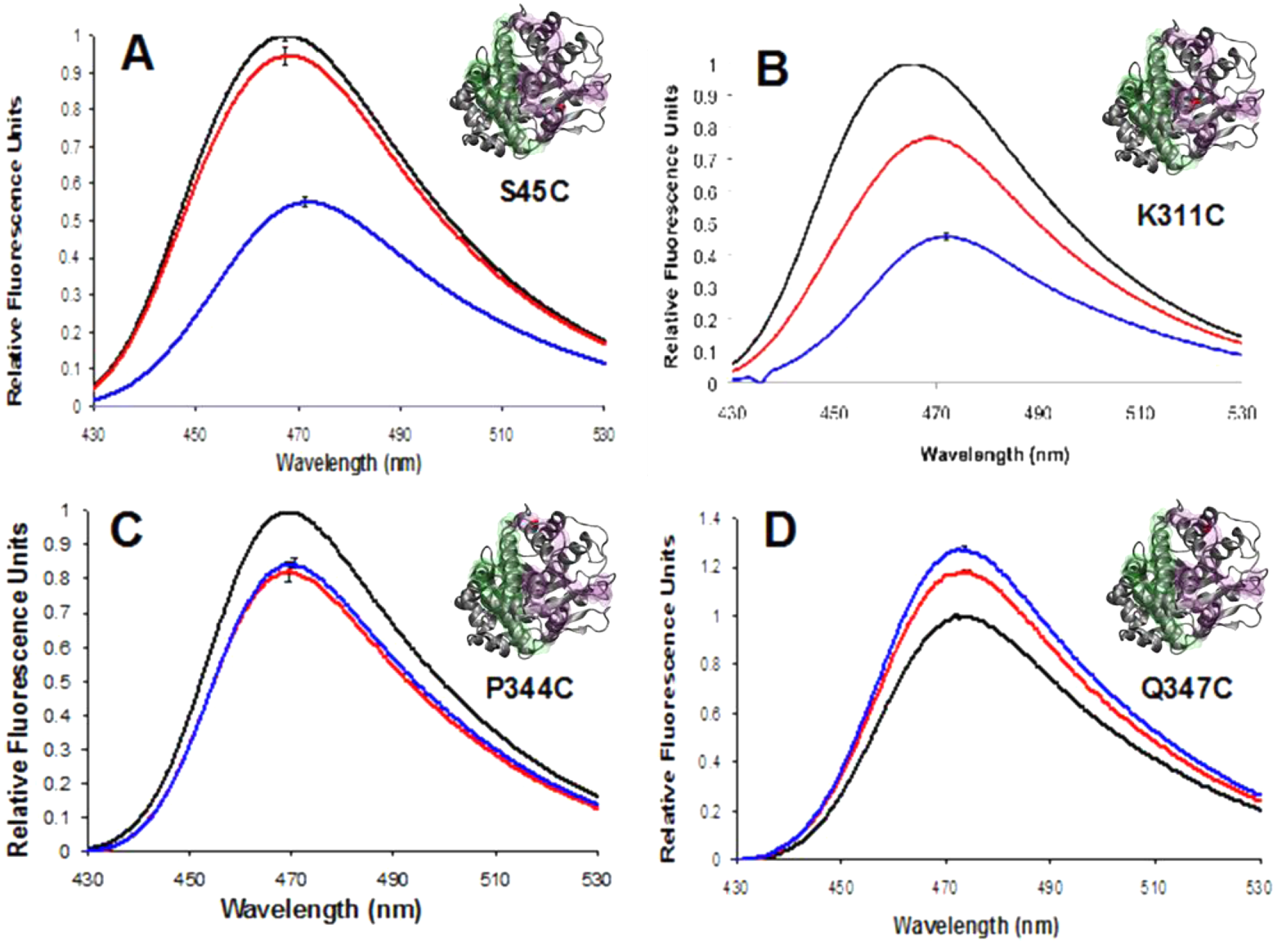


**Figure 3.** Fluorescence emission spectra of MDCC-labeled variants in the TSP. The emission spectra of the fluorescently labeled proteins are shown for the conditions no substrate (black), Fru 1,6-$P_2$ (blue), and Fru 1-P (red). (A) S45C, (B) K311C, (C) P344C, and (D) Q347C. Insets are monomeric structures as depicted in Figure 1 except with only the particular variant indicated as appropriate for each spectrum. Substrates were used at concentrations of 0.5 mM for Fru 1,6-$P_2$, and 10 mM for Fru 1-P. Enzyme concentration was (0.5 $\mu$M). Spectra were normalized to the maximum emission signal of the no substrate condition for each variant to give relative fluorescence units (RFU). Errors noted by bars at the emission maxima are given as 1 SD.

(Fru-1,6-$P_2$ and Fru-1-P $k_{cat}/K_m$ values), including no significant changes in the ratio of efficiencies toward these two substrates (Table S2). Incorporation of these surface cysteine residues did not drastically change the isozyme-specific kinetic properties of these aldolase A variants.

Each aldolase single Cys-variant was labeled with MDCC with a labeling efficiency between 50 and 100% (Table S3) and was tested for changes in activity due to labeling. The labeled variants retained their $k_{cat}$ values (variants were ±25% compared to wild type) and showed slight increases in $K_m$ values (<4−7-fold) (Table S3). These data indicated that variants adducted with the MDCC fluorophore had only modest changes in overall catalytic activity (<5-fold changes in $k_{cat}/K_m$ values). It was determined that unlabeled material did not affect the fluorescence signal (data not shown) so it was not separated from the labeled material for subsequent assays.

Four variants of the DSP (F57C, A72C, L320C, V328C) were used to test the substrate-dependent conformational change hypothesis. The DSP is furthest from the active site and not associated with any known regions of conformational flexibility from crystal structures, or from enzyme flexibility as assessed by temperature factors (B-values). The emission spectrum of each fluorescently labeled enzyme was measured with and without either Fru 1,6-$P_2$ or Fru 1-P and performed in a time frame such that equilibrium was reached (Figure 2). All enzymes showed decreased intensities in their fluorescence emission spectra in the presence of at least one substrate, which was consistent with a substrate-dependent conformational change. Furthermore, the spectra were different depending on which substrate was present, with consistently smaller effects in the presence of Fru 1-P, with the exception of MDCC-labeled L320C toward Fru 1-P, in which the spectrum was unchanged from that with no substrate. The same experiment was performed on the MDCC-labeled S131C variant, which had the Cys substitution on an $\alpha$-helix that is not part of either the DSP or the TSP. No change in fluorescence emission was observed with either substrate for MDCC-labeled S131C, which confirmed that substrate-dependent fluorescence changes were specific to the DSP. The observed degree of fluorescence change and red shifts in maximum wavelength of fluorescence emission in the presence of both substrates are tabulated in Table S4. The variant F57C showed the largest decrease in fluorescence intensity in the presence of Fru 1,6-$P_2$ accompanied by a redshift (Figure 2A). The variants A72C and V328C each showed a smaller fluorescence decrease than F57C in the presence of Fru 1,6-$P_2$, but slightly larger decreases than


DOI: 10.1021/jacs.5b08149
J. Am. Chem. Soc. 2015, 137, 13876−13886

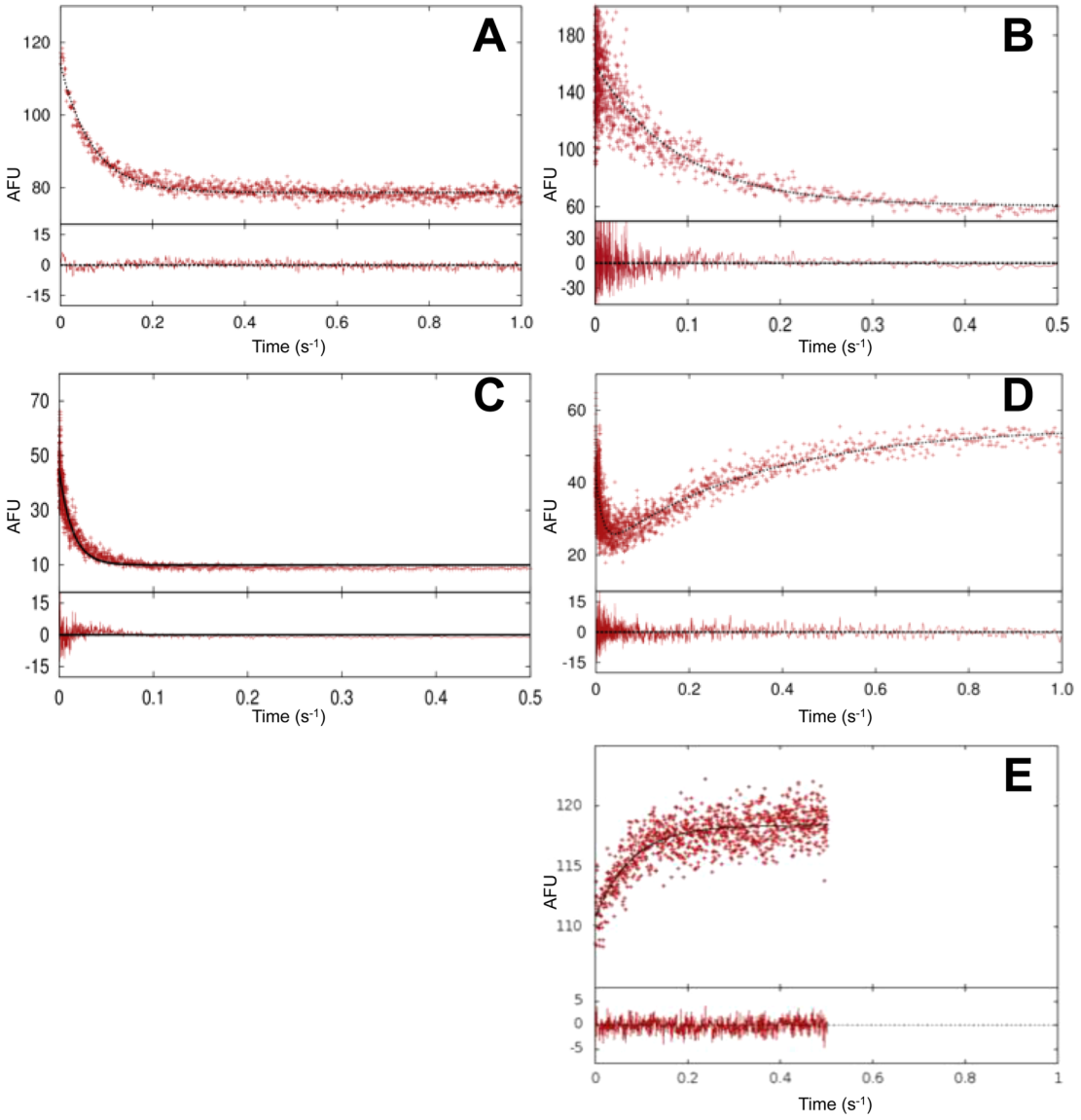


**Figure 4.** Representative stopped-flow emission kinetics for DSP and TSP aldolase variants. Representative stopped-flow emission plots of arbitrary fluorescence units (AFU) versus time after rapid mixing with 500 $\mu$M Fru 1,6-$P_2$ are shown for F57C (A) and V328C (B) in the DSP, S45C (C) and K311C (D) in the TSP, and AFU versus time after rapid mixing with 50 mM Fru 1-P and K311C (E). Enzyme concentration was (0.25 $\mu$M). The top plots show raw data (dots) and best-fit kinetic models. Bottom plots show residuals. Data were collected on either a Hi-Tech KinetAsyst Stopped-Flow System or an Applied Photophysics DX.17MV instrument equipped with the Pro-Data upgrade and an emission photomultiplier tube using a 420 nm filter. The kinetic parameter fittings were performed with DYNAFIT.[32]

in the presence of Fru 1-P (Figure 2B,D). The variant L320C showed no spectral change in the presence of Fru 1-P, but did show a slight decrease in the presence of Fru 1,6-$P_2$ (Figure 2C). These results are consistent with a substrate-dependent conformational change in the region of the DSP, which lead to the observed fluorescence change.

Given that fluorescence changes in the DSP were evident upon substrate binding, and that these fluorescence changes were apparently different depending on the substrate, the question arises whether similar changes could be observed in the TSP that would explain the known cooperativity of these two regions in determining the substrate specificity of aldolase A.[17] Four labeled variants in the TSP (S45C, K311C, P344C and Q347C) were tested for comparable substrate-dependent conformational changes to those of the DSP-labeled enzymes. The emission spectrum of each fluorescently labeled enzyme was measured with and without either Fru 1,6-$P_2$ or Fru 1-P (Figure 3). The variant S45C showed a large fluorescence decrease and redshift in the presence of Fru 1,6-$P_2$, and almost no change in the presence of Fru 1-P (Figure 3A). The variant K311C showed a large fluorescence decrease in the presence of both substrates, but the magnitude of the change was greater with Fru 1,6-$P_2$ than with Fru 1-P (Figure 3B). The two variants in the C-terminal region, which is known to undergo conformational changes associated with activity,[21,22,31] were distinctly different than the other spectra. The variant P344C showed the same fluorescence decrease regardless of the substrate (Figure 3C). The variant Q347C showed an increase in fluorescence that was slightly lower in magnitude with Fru 1-P than with Fru 1,6-$P_2$ (Figure 3D). The observed degree of fluorescence emission change of reporters in the TSP and red shifts in maximum wavelength in the presence of both substrates are tabulated in Table S4. Notably, there was no correlation between the magnitude of the fluorescence changes


DOI: 10.1021/jacs.5b08149
J. Am. Chem. Soc. 2015, 137, 13876−13886

and the distances from the substrate phosphates to the fluorophores (Figure S1); this rules out some trivial explanations regarding these observed changes in fluorescence; one, that electrostatic effects on the quantum yield are due to attracting or repelling some quenching molecules, or two, that electrostatics differentially changed the dielectric, which would could cause a change in the energy level difference and corresponding shift of the emission peak. These changes in spectra for the CTR variants were consistent with a nonsubstrate-distinct and requisite conformational change in the CTR during catalysis as part of the second half-reaction that includes the rate-limiting step with either substrate. In contrast, clear differences between substrates were shown in the spectral changes of enzymes with the fluorophore on $\alpha$-helices that flank the substrate-binding site (S45C and K311C).

**Fluorescence Changes Occur on the Time Scale of Catalysis.** If the substrate-dependent changes in fluorescence were due to substrate-specific conformational changes, then the time-scale of the fluorescent change after binding substrate should be within the time scale of the catalytic cycle. Stopped-flow fluorescence spectrophotometry was performed on those variants with substantial differences in fluorescence intensity with and without substrate at equilibrium (>20%). These variants were F57C and V328C in the DSP (see Figure 2), and S45C and K311C in the TSP (see Figure 3). The decreases in fluorescence intensity versus time for each of these variants are shown in Figure 4A–D. All variants were fit to multiple kinetic models (Figure S2A) and the best-fit models for each used to determine the rate constants of fluorescence changes (Table 1).

**Table 1. Observed Rates of Substrate-Dependent Fluorescence Change**

| variant | ISR patch | $k_{cat}$[b] ($s^{-1}$) | Fru 1,6-$P_2$ (500 $\mu$M) $k_{obs}$[a] ($s^{-1}$) | Fru 1-P (50 mM) $k_{obs}$[a] ($s^{-1}$) |
|---|---|---|---|---|
| F57C | DSP | 0.7 | 17 | ND[c] |
| V328C | DSP | 0.9 | 9 | ND |
| S45C | TSP | 0.9 | 72 | ND |
| K311C | TSP | 0.93 | 63 ($k_2$ = 3.4) | 32 |

[a]All rates were determined at 4 °C. [b]Determined for Fru 1,6-$P_2$ at 30 °C using steady-state kinetics and corrected to 4 °C using Arrhenius equation (see Table S4). [c]Not determined.

The two variants in the DSP fit best to a single decay model and had similar fluorescent decay time constants (~15 $s^{-1}$) (Figure 4A,B). The two variants in the TSP both have initial fluorescence decay rates faster than those in the DSP (~70 $s^{-1}$) (Figure 4C,D). Notably, the K311C variant showed a second, slower fluorescent event (3.4 $s^{-1}$) and had an optimal fit to a sequential three-state scheme (Figure S2B, Models 3 and 4). Importantly, all the rate constants for the first step were of the same order of magnitude or faster than catalytic turnover ($k_{cat}$ ~ 1 $s^{-1}$ for Fru 1,6-$P_2$[9,11]). Consistent with this correlation, the same experiments performed using the negative control, MDCC-labeled S131C, showed no time-dependent change in fluorescence (data not shown), as expected from the results of the equilibrium emission spectra (see Figure 2E). These kinetic data are consistent with the direct involvement of the TSP and DSP in cooperative conformational changes important for catalysis of Fru 1,6-$P_2$.[17]

Given the notable biphasic behavior of the MDCC-labeled K311C with Fru 1,6-$P_2$ (Figure 4D) and its substantial change with Fru 1-P at equilibrium (see Figure 3B), it was used to monitor the rate of fluorescence change with Fru 1-P. The kinetic behavior was again consistent with the time scale of catalysis with an exponential observed rate of 32 $s^{-1}$ (Table 1); however, the biphasic changes were not seen with Fru 1-P (Figure 4E). Instead, K311C showed an increase in fluorescence with Fru 1-P at a time scale consistent with a change occurring in the first half-reaction. This difference in fluorescence behavior for Fru 1-P versus Fru 1,6-$P_2$ is a clear indication that different enzyme conformations are elicited by each of the two aldolase substrates.

**Fluorescence Changes Indicate Substrate Binding.** The fluorescence changes described above are consistent with conformational changes in the DSP and TSP upon substrate binding and catalysis. This model would predict a dependence of fluorescence change on substrate concentration. The variants that showed the greatest degree of fluorescence intensity change between the two substrates were F57C, in the DSP, and both S45C and K311C in the TSP (Figure 2A, 3A, and 3B, respectively). These three variants were used to show dependence of the fluorescence change on the substrate concentration. The emission spectra of the labeled variants were measured over a range of concentrations for each substrate (Figure S3). Plotting the fluorescence maximum as a function of substrate concentration showed a clear hyperbolic dependence for MDCC-labeled F57C, S45C, and K311C for Fru 1,6-$P_2$ and Fru 1-P (Figure S4). The apparent $K_{conf}$ values were derived from fitting to a two-state equilibrium and are compared to $K_m$ values of each variant in Table 2. The $K_{conf}$ values appear to report on substrate-induced effects with values similar to their respective $K_m$ values for each substrate, with two significant differences. For Fru 1,6-$P_2$, this value for the TSP representative (S45C) was significantly smaller value than $K_m$. Likewise, for Fru 1-P, the fluorescence changes monitored by the fluorophore at F57C, which is a surrogate for the DSP, had significantly smaller value of $K_{conf}$ than the value for $K_m$. These differences in $K_{conf}$ values may represent more specific steps in catalysis of each substrate that are different than the conglomerate series of steps reported through the $K_m$ values.[21] Taken together, the analysis of fluorescence spectral changes among the MDCC-labeled aldolase variants involving the DSP and TSP clearly report on conformational changes in binding and catalysis that differ depending on the substrate encountered.

**Table 2. Apparent Equilibrium Constants for Conformational Changes ($K_{conf}$) Due to Substrate-Binding As Detected by Fluorescence Changes**

| | | Fru 1,6-$P_2$ ($\mu$M) | | Fru 1-P (mM) | |
|---|---|---|---|---|---|
| variant | ISR patch | $K_m$[a] | $K_{conf}$[b] | $K_m$[a] | $K_{conf}$[b] |
| F57C | DSP | 38 ± 0.5 | 70 ± 7 | 23 ± 6 | 1.9 ± 0.9 |
| S45C | TSP | 32 ± 0.4 | 7.5 ± 1.9 | 10 ± 0.5 | 11 ± 5 |
| K311C | TSP | 35 ± 0.6 | 62 ± 13 | 10 ± 1.4 | 4.6 ± 1 |

[a]From Table S2. [b]Values from fitting hyperbolic equations to plots of concentration dependent changes in $\lambda_{max}$ for fluorescence spectra. Errors are SEM for several determinations for each variant with each substrate. Supporting Information shows representative spectra (Figure S3) and plots (Figure S4).

Lastly, the K311C-labeled variant showed a fluorescence change with a rate similar to that of turnover for Fru 1,6-$P_2$ (3.4 $s^{-1}$ vs. $k_{cat}$ = ~1 $s^{-1}$), thus indicating that it reflects the rate-limiting step. In addition, the second half-reaction should be


DOI: 10.1021/jacs.5b08149
J. Am. Chem. Soc. 2015, 137, 13876–13886

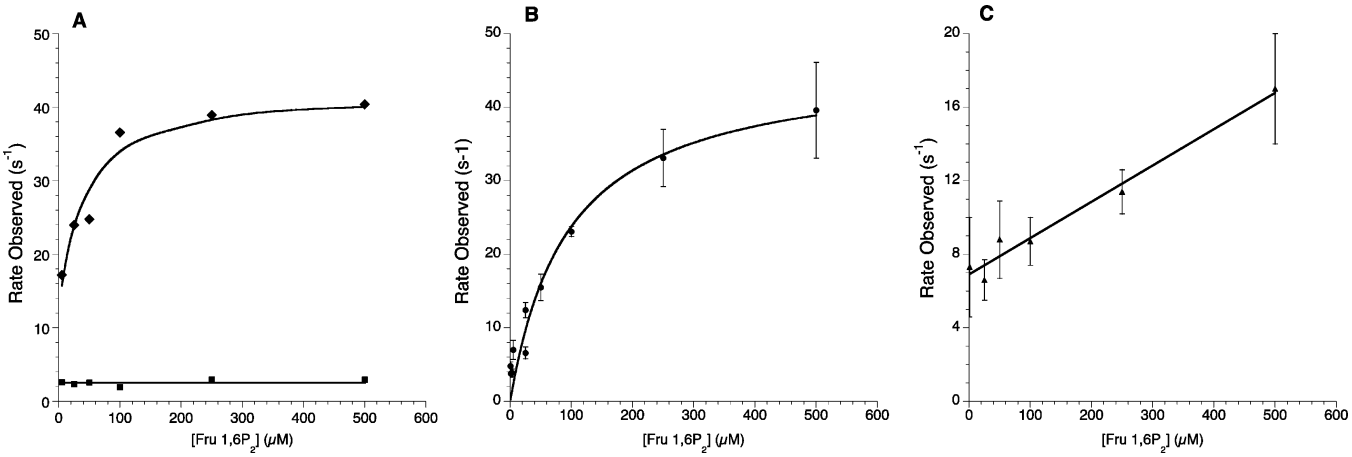


**Figure 5.** Observed rates of fluorescence change as a function of substrate concentration for DSP versus TSP. (A) Plots of first order observed rates for the fluorescence change as a function of concentration of Fru 1,6-$P_2$ for the fast (◆) and slow (■) kinetic steps observed in variant K311C (enzyme concentration was 0.25 $\mu$M) in the TSP. The concentration dependence of the rate constant for the fast step of K311C was fit to a hyperbolic model for ligand binding ($R^2$ = 0.94). (B) As in (A), but for S45C (●) in the TSP and fit to a hyperbolic model for ligand binding ($R^2$ = 0.95). (C) As in (A), but for F57C (▲) in the DSP and fit to a linear model for ligand binding ($R^2$ = 0.94). Models used for the analysis are shown in Figure S5.

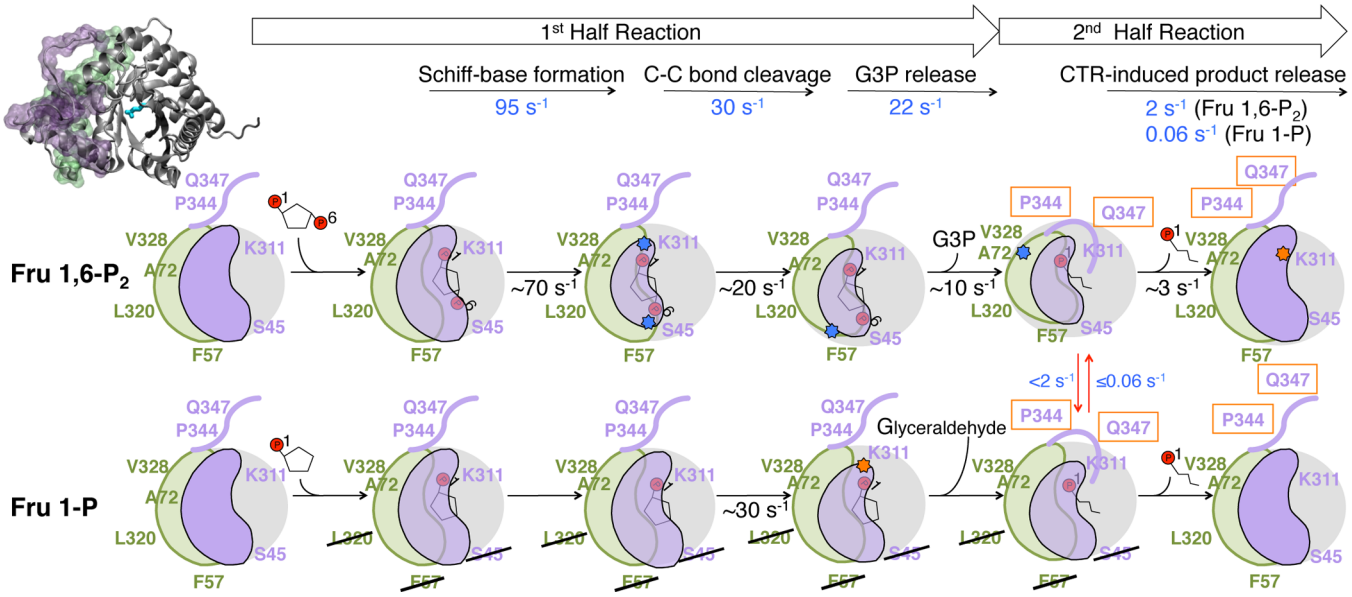


**Figure 6.** Schematic summary of substrate-induced conformational changes during the aldolase cleavage reactions. At top, the boxed arrows indicate the two half reactions, below which are steps in catalysis with the published rates of the indicated reactions adjusted to 4 °C[11,13] (see also Table S5). At top left is a color-coded ribbon structure (see Figure 1) where the DSP (green) and TSP (purple) are indicated. In the cartoon, aldolase monomer is represented as a sphere (gray) with the CTR as a tail. The regions and residues used for fluorophore adduction are indicated for the DSP and TSP with the same color code as in the ribbon diagram. Below the arrows are the rates of substrate-induced fluorescence changes (see Table 1) for each substrate. The two substrates are shown with a schematic indicating C1- and C6-phosphates by numbered "P"s in red circles. Changes in conformation of DSP or TSP are indicated by size changes in the lobes of DSP/TSP cartoon. For those residues with measured rates of fluorescence change (see Table 1), a star is shown (losses in blue and increases in orange). Residues not reporting significantly large changes in fluorescence spectra in the presence of Fur 1-P are indicated with a slash through the name. Residues reporting the same fluorescence spectral change regardless of substrate are boxed in orange. Double-red arrows indicate a hypothetical equilibrium between the second half-reaction conformers.

substrate independent. So, the rate of this slower fluorescence change was measured as a function of Fru 1,6-$P_2$ (1−500 $\mu$M). The plot shown in Figure 5A (squares) clearly shows that the rate of this change was independent of substrate.

For those variants where there was a >20% change in fluorescence intensity (F57C in the DSP and S45C and K311C in the TSP), the dependence of the observed rate on the substrate concentration determined from stop-flow experiments was measured (Figure 5). For K311C, the fast observed rate versus [S] fit a hyperbolic equation (Figure 5A), which is consistent with a rapid equilibrium followed by a slower reaction (Figure S5, model 3). For S45C, there is a similar observation as for the fast rate of K311C (Figure 5B). For F57C there was a linear dependence of the observed rate versus [S] (Figure 5C), which is consistent with a simple binding equilibrium (Figure S5, model 2). The fact that both K311C


DOI: 10.1021/jacs.5b08149
J. Am. Chem. Soc. 2015, 137, 13876−13886

and S45C are in the TSP and show similar concentration-dependence of the observed rates indicated that they report on that same conformational event(s); either limited by substrate binding or associated with binding. The maximum value for the rate constants (63 and 72 $s^{-1}$) is consistent with a step that occurs in the first half-reaction but is slower than Schiff-base formation (100 $s^{-1}$)[11,13] and still dependent on the substrate concentration, either C−C bond cleavage or G3P release. This result indicated that all steps in the first half reaction are dependent on substrate concentration.

## DISCUSSION

Recent research into enzyme structural flexibility has highlighted the importance of conformational changes distant from the active site on catalysis. These conformational changes have been shown to affect rates of catalysis in enzymes such as DHFR and proline isomerase, and in enzymes such as T7 DNA polymerase, these alternate conformations have been shown to impact substrate specificity.[2,8,33] T7 DNA polymerase has shown that the enzyme adopts different conformations upon binding either matching or mismatching nucleotides.[2] Understanding these alternate conformations and their role in catalysis is tantamount to obtaining a complete picture of enzyme catalysis and is possible only with an integrative approach to discovering these conformations and how they affect function. In aldolase, by observing conformational changes at multiple sites known to be important for substrate specificity,[34] a picture of how the enzyme uses these conformational changes subsequent to substrate binding has emerged.

Single cysteine variants selectively placed within the DSP and TSP, were fluorescently labeled, and used to probe the alternate conformations of the protein in the presence of both Fru 1-P and Fru 1,6-$P_2$. These studies suggested that almost all the variants adopted alternate conformations depending on which substrate was bound as evidenced by the different emission patterns observed for each substrate, and that changes in conformation were faster than turnover. Importantly, these alternate conformations were constrained to the regions previously identified in substrate-specific conformational changes (i.e., no fluorescence changes shown for the S131C control). Taken together, the results suggest a model for how these conformational changes are involved in the catalytic cycle.

**Model of Conformational Changes in the Aldolase Catalytic Mechanism.** If the substrate-induced fluorescence changes for all the MDCC-labeled aldolase variants were due to conformational changes in the regions where the fluorophores were located, then a series of events in the catalytic cycle can be described. These events explain the apparent paradox of how different kinetic values for Fru 1,6-$P_2$ vs Fru 1-P among vertebrate Fru 1,6-$P_2$ aldolases are manifest in the rate-limiting second half-reaction even though the second half-reaction is identical for both substrates (see Scheme 1). The 10-fold faster $k_{cat}$ value for Fru 1,6-$P_2$ versus Fru 1-P seen for aldolase A would only require a subtle energetic difference (less than −6 kJ/mol),[35] and the difference may lie in the interactions due to conformational changes of the DSP and TSP as revealed in this study.

A model that is consistent with the fluorescence data and the coupling between the TSP and DSP patches[17] was developed to explain how binding differences between hexoses are propagated through conformational changes to set up product release, which controls the value of $k_{cat}$ (Figure 6).[12,13] Furthermore, the conformational-change model was favored over any model involving electrostatic effects because there was no correlation between observed fluorescence changes for the mono- versus bis-phosphorylated substrates and distance between the labeled residue and the two phosphate binding sites (see Figure S1). It should be noted that the proposed model shows (Figure 6) the events measured by fluorescence in the first half-reaction (K311C, S45C, and F57C) as separate events since the measured rates correlated well to rates previously measured for these steps (Schiff base formation, C−C bond cleavage, and G3P release). However, it is possible that the fluorescence events do not report on these discrete steps and what was observed in the fluorescence changes is an average of several steps in the first half reaction.

The events leading to the faster catalytic rate for Fru 1,6-$P_2$ can be hypothesized on the basis of these results (Figure 6). The MDCC-labeled S45C variant ($\alpha$-helix 2 in the TSP) was observed to have the fastest (see Table 1) and one of the largest (see Figure 3A) of the fluorescence changes. From crystallographic and mutagenic data it has previously been suggested that the conserved residues Lys41 and Arg42 in $\alpha$-helix 2 directly interact with the C6-phosphate of Fru 1,6-$P_2$.[18,36] The rate of the fluorescence change observed for $\alpha$-helix 2, reported by the S45C-variant, after binding the C6-phosphate was similar to the rate of Schiff-base formation (~100 $s^{-1}$).[13] On the other side of the active site in the TSP is $\alpha$-helix 13, reported by the K311C-labeled variant. The relatively fast initial change in fluorescence for this variant in the presence of Fru 1,6-$P_2$, was also similar to the rate of Schiff-base formation. For both $\alpha$-helices 2 and 13, changes in conformation must be cotemporal with events of the first half reaction.[11]

The next event is the propagation of this movement to $\alpha$-helix 3 in the DSP, which is reported by the MDCC-labeled F57C variant. This variant showed the next greatest fluorescence change (see Figure 2A) at a slower rate of 17 $s^{-1}$ (see Table 1). Next, the long $\alpha$-helix 14 in the DSP, is reported by MDCC-labeled V328C, and had an even slower rate of fluorescence change (9 vs 17 $s^{-1}$). The conformational changes from $\alpha$-helix 3 to $\alpha$-helix 14 are propagated through $\alpha$-helix 4, which lies between these two helices, and shows a fluorescence change reported by the MDCC-labeled A72C variant (rates were not measured for A72C, but the magnitude of fluorescence change was similar to that for V238C). The rates of these conformational changes were similar to those for carbon−carbon bond cleavage (30 $s^{-1}$)[13] and G3P release (22 $s^{-1}$),[37] which ends the first half-reaction, suggesting that the F57C, A72C, and V328C variants report on these events.

The results from previous studies as well as the magnitudes of the fluorescence changes shown here are consistent with a final step being the propagation of conformational changes to the CTR. The repositioning of this region has been implicated in the rate-limiting step of DHAP release.[22,31] The CTR is critical for enamine protonation by the terminal Tyr363 and rate-limiting product release in the second half-reaction.[31] Although many explanations for the magnitude of fluorescence changes in the spectra are possible, in this case, if the degree of fluorescence change reflects the degree of conformational change, it is consistent with a ripple effect initiated by binding to the C6-phosphate. The largest perturbation was in the reporter for $\alpha$-helix 2 (S45C), followed by $\alpha$-helix 3 (F57C), then $\alpha$-helix 4 (A72C), then $\alpha$-helix 14 and the CTR (V328C, Q347C, and P344C). The lone inconsistency with this correlation was the lower degree of fluorescence change for


DOI: 10.1021/jacs.5b08149
J. Am. Chem. Soc. 2015, 137, 13876−13886

MDCC-labeled L320C (see Figure 2C) than that for MDCC-labeled V328C (both in $\alpha$-helix 14), but since the observed changes in fluoresence are affected by both the magnitude of conformational changes as well as relative positioning of the fluorophore, the magnitude of change need not necessarily correlate.

In addition to the CTR, another element in the TSP, reported by the MDCC-labeled K311C variant in $\alpha$-helix 13, showed a second slower phase of fluorescence change that had a rate essentially the same as turnover ($k_{cat}$ value at 4 °C is ~1 $s^{-1}$),[11,13] which governs by the second half reaction. The lack of substrate dependence of this second fluorescence event (see Figure 5) is consistent with events in the second half reaction.

While these events in the presence of Fru 1,6-$P_2$ are revealing, events differ in the presence of Fru 1-P. In a similar fashion, the events leading to the slower catalytic rate of turnover for Fru 1-P can be hypothesized. First, the fluorescence changes initiated by C6-phosphate binding described above for Fru 1,6-$P_2$ were not seen with Fru 1-P for MDCC-labeled S45C, F57C, and L320C; see Figures 3A, 2A, and 2C, respectively). Moreover, the rate of change reported by K311C was not biphasic with Fru 1-P as it was for Fru 1,6-$P_2$ and occurred at a distinctly different rate (32 $s^{-1}$). This leads to the conclusion that the conformational changes undergone upon Fru-1-P binding differ significantly from those undergone upon Fru-1,6-$P_2$ binding, likely due to differing effects on $\alpha$-helix 2 due to the lack of the C6 phosphate on the substrate. The propagation of this conformational change to the CTR by $\alpha$ helix 13 reported by MDCC-labeled K311C with Fru 1-P may result simply in a different rate of change to the CTR necessary for catalysis during the second half-reaction. This is supported by the very similar fluorescence changes shown for MDCC-labeled P344C (diminution) and Q347C (enhancement) for either substrate (see Figure 3C−D).

Although the exact structural elements and their motions are not defined here, it is clear that there was a distinct set of conformational changes in the presence of Fru 1-P when compared to Fru 1,6-$P_2$. The rate-determining step in the second half reaction can therefore be ascribed to either the release of DHAP (at the rate of 2 $s^{-1}$ for Fru 1,6-$P_2$ versus 0.06 $s^{-1}$ for Fru 1-P) or in the case of Fru 1-P the rate of a slow conversion of the DHAP-bound conformer from that set up by Fru-1-P cleavage to that set up by Fru-1,6-$P_2$ cleavage (noted by the red arrows in Figure 6). Regardless of which pathway, this clearly supports the hypothesis of differential dynamics due to different substrates. The differential effects of substrate on $\alpha$-helix 13 appear to be key to understanding this distinction.

Dissecting the mechanism of substrate specificity is an important question in enzymology, because many enzymes have multiple substrates among which they must choose for proper cell function. Many enzymes are present in the form of isozymes, which differ only slightly, but these differences allow them to serve different functions in the cell. For many of these isozymes, it is reasonable that the few differences in amino acids, which often do not contribute noticeably to differences in the static structure or active site,[19] could be causing differences in dynamics of certain regions.

In studies over the past decade, the concept that substrate-induced conformational changes can be a major determinant of enzyme specificity has been put forward[38] based on analysis of T7 DNA polymerase.[2] Changes in conformation correlated with differences in substrate specificity have also been described for DHFR and proline isomerase.[8,33] For the DNA polymerase, binding of a correct nucleotide is followed by a favorable isomerization and a fast polymerization rate. The specificity constant for correct nucleotide incorporation is governed by the nucleotide affinity in the initial weak binding to an "open" state and the rate of the conformational change to form a "closed state." This observation is also consistent with molecular dynamics simulations.[8,33,39] Moreover, selection against a mismatched nucleotide involves an initial thermodynamic selection with a significant decrease in affinity, followed by kinetic control resulting from a decrease in the rate of the chemical step. Similar mechanisms have been proposed in Class II aminoacyl-tRNA synthetase[40] for which it has been shown that tRNA selection arises from interactions between tRNA and the active site that provide kinetic discrimination at distinct points in the catalytic cycle. Similarly, selection of the cognate aminoacyl tRNA on the ribosome is kinetically controlled via GTPase rates versus noncognate substrates.[41] Both aminoacyl-tRNA synthetase and the translation machinery presumably affect this kinetic discrimination via associated conformational changes, but it is difficult to measure these structure-based mechanisms directly. In the case detailed here for Fru-1,6-$P_2$ aldolase, different conformational states promoted by binding alternate substrates were clearly detected and these states were occupied at rates consistent with steps in the catalytic cycle. Thus, the enzyme is set on two alternative paths, depending on the substrate encountered.

## CONCLUSIONS

In these studies, not only whether, but also how, enzyme conformational changes and dynamics are involved in substrate specificity has been delineated. These conformational changes have been pinpointed to the regions of the enzyme undergoing these changes and correlated with step(s) in the catalytic cycle, demonstrating their effect on steps that are responsible for both the $K_m$ and $k_{cat}$ values of the different substrates. The key to these discoveries was the recognition of the evolutionary conservation of isozyme specific residues and the design of conformationally sensitive fluorophores near these residues. Using fluorescence spectroscopy in the presence or absence of two physiological aldolase substrates; Fru 1,6-$P_2$ or Fru 1-P, differences in the magnitude and rates of fluorescence change suggested a mechanism by which aldolase substrate specificity is conferred by differential conformational changes. These data unveiled details well beyond a simple induced fit model and have indicated that binding events for the two fructose substrates are linked to distinct downstream conformational changes responsible for different rate limiting steps, including the last step of product release. Thus, aldolase distinguishes between substrates by differing substrate-triggered conformational changes.

## ASSOCIATED CONTENT

### Supporting Information

The Supporting Information is available free of charge on the ACS Publications website at DOI: 10.1021/jacs.5b08149.

A table of DTNB reactivity, three tables of kinetic measurements for these variants, one table summarizing the fluorescence data, one table summarizing rates of intermediate reactions during catalysis, a figure showing lack of correlation of fluorescence with phosphate groups, a figure fitting stopped-flow data to various kinetic models, two figures detailing the fluorescence



DOI: 10.1021/jacs.5b08149
J. Am. Chem. Soc. 2015, 137, 13876−13886

changes and [substrate], and a figure of kinetic schemes and associated equations for plotting [substrate] versus stopped-flow rate data. (PDF)

## AUTHOR INFORMATION


### Corresponding Authors

*tolan@bu.edu

*drkallen@bu.edu

### Present Addresses

[⊥]Novartis Institutes for Biomedical Research, Cambridge, Massachusetts 02139, United States.

[∥]University of California at San Francisco, School of Pharmacy, Dept. of Bioengineering and Therapeutic Sciences MC2552, Mission Bay, Byers Hall, 1700 Fourth Street, Suite 503B, San Francisco, California 94158-2330, United States.


### Notes

The authors declare no competing financial interest.

## ACKNOWLEDGMENTS

We thank Drs. John Caradonna and Joanne Stubbe for the use of their stopped-flow instruments. We thank Dr. Adrian Whitty for critical reading of the manuscript and helpful suggestions. We thank the early contributions of Elizabeth Brunyak and Dr. John Pezza. An award from the Arnold & Mabel Beckman Foundation Scholars Program supported Florencia Rago.

## REFERENCES


(1) (a) Levitzki, A.; Koshland, D. E., Jr. *Biochemistry* **1972**, *11*, 247−253. (b) Haldane, J. B. S. *The Causes of Evolution*; Longmans and Green: London, 1932.

(2) Tsai, Y. C.; Johnson, K. A. *Biochemistry* **2006**, *45*, 9675−9687.

(3) (a) Kern, D.; Zuiderweg, E. R. *Curr. Opin. Struct. Biol.* **2003**, *13*, 748−757. (b) Henzler-Wildman, K. A.; Thai, V.; Lei, M.; Ott, M.; Wolf-Watz, M.; Fenn, T.; Pozharski, E.; Wilson, M. A.; Petsko, G. A.; Karplus, M.; Hubner, C. G.; Kern, D. *Nature* **2007**, *450*, 838−844. (c) Benkovic, S. J.; Hammes-Schiffer, S. *Science* **2003**, *301*, 1196−1202.

(4) Hammes-Schiffer, S.; Benkovic, S. J. *Annu. Rev. Biochem.* **2006**, *75*, 519−541.

(5) Boehr, D. D.; McElheny, D.; Dyson, H. J.; Wright, P. E. *Proc. Natl. Acad. Sci. U. S. A.* **2010**, *107*, 1373−1378.

(6) Schnell, J. R.; Dyson, H. J.; Wright, P. E. *Annu. Rev. Biophys. Biomol. Struct.* **2004**, *33*, 119−140.

(7) (a) Miller, G. P.; Benkovic, S. J. *Chem. Biol.* **1998**, *5*, R105−R113. (b) Huang, Z.; Wagner, C. R.; Benkovic, S. J. *Biochemistry* **1994**, *33*, 11576−11585. (c) Liang, Z. X.; Tsigos, I.; Lee, T.; Bouriotis, V.; Resing, K. A.; Ahn, N. G.; Klinman, J. P. *Biochemistry* **2004**, *43*, 14676−14683. (d) Liang, Z. X.; Lee, T.; Resing, K. A.; Ahn, N. G.; Klinman, J. P. *Proc. Natl. Acad. Sci. U. S. A.* **2004**, *101*, 9556−9561. (e) Liang, Z. X.; Klinman, J. P. *Curr. Opin. Struct. Biol.* **2004**, *14*, 648−655.

(8) Fraser, J. S.; Clarkson, M. W.; Degnan, S. C.; Erion, R.; Kern, D.; Alber, T. *Nature* **2009**, *462*, 669−673.

(9) Penhoet, E. E.; Rutter, W. J. *J. Biol. Chem.* **1971**, *246*, 318−323.

(10) Rose, I. A.; O'Connell, E. L.; Mehler, A. H. *J. Biol. Chem.* **1965**, *240*, 1758−1765.

(11) Choi, K.-H.; Tolan, D. R. *J. Am. Chem. Soc.* **2004**, *126*, 3402−3403.

(12) Rose, I. A.; Warms, J. V. B.; Kuo, D. J. *J. Biol. Chem.* **1987**, *262*, 692−701.

(13) Morris, A. J.; Tolan, D. R. *Biochemistry* **1994**, *33*, 12291−12297.

(14) This rate limiting step for Fru 1-P can be inferred from studies of aldolase B, where it has the same rate as aldolase A for the faster first half-reaction for Fru-1,6-$P_2$ cleavage, yet the two substrates have identical $k_{cat}$ values.[11]

(15) (a) Kochman, M.; Dobryszycki, P. *Acta Biochim. Polym.* **1991**, *38*, 407−421. (b) Heyduk, T.; Michalczyk, R.; Kochman, M. *J. Biol. Chem.* **1991**, *266*, 15650−15655.

(16) Kobashi, K.; Horecker, B. L. *Arch. Biochem. Biophys.* **1967**, *121*, 178−186.

(17) Pezza, J. A.; Stopa, J. D.; Brunyak, E. M.; Allen, K. N.; Tolan, D. R. *Biochemistry* **2007**, *46*, 13010−13018.

(18) Choi, K. H.; Shi, J.; Hopkins, C. E.; Tolan, D. R.; Allen, K. N. *Biochemistry* **2001**, *40*, 13868−13875.

(19) Arakaki, T. L.; Pezza, J. A.; Cronin, M. A.; Hopkins, C. E.; Zimmer, D. B.; Tolan, D. R.; Allen, K. N. *Protein Sci.* **2004**, *13*, 3077−3084.

(20) (a) Dalby, A.; Tolan, D. R.; Littlechild, J. A. *Acta Crystallogr., Sect. D: Biol. Crystallogr.* **2001**, *57*, 1526−1533. (b) Sygusch, J.; Beaudry, D.; Allaire, M. *Proc. Natl. Acad. Sci. U. S. A.* **1987**, *84*, 7846−7850.

(21) Berthiaume, L.; Tolan, D. R.; Sygusch, J. *J. Biol. Chem.* **1993**, *268*, 10826−10835.

(22) Blom, N.; Sygusch, J. *Nat. Struct. Biol.* **1997**, *4*, 36−39.

(23) Pezza, J. A.; Choi, K. H.; Berardini, T. Z.; Beernink, P. T.; Allen, K. N.; Tolan, D. R. *J. Biol. Chem.* **2003**, *278*, 17307−17313.

(24) Ho, S.; Hunt, H.; Horton, R.; Pullen, J.; Pease, L. *Gene* **1989**, *77*, 51−59.

(25) Beernink, P. T.; Tolan, D. R. *Protein Expression Purif.* **1992**, *3*, 332−336.

(26) Morris, A. J.; Tolan, D. R. *J. Biol. Chem.* **1993**, *268*, 1095−1100.

(27) Racker, E. *J. Biol. Chem.* **1947**, *167*, 843−854.

(28) Bradford, M. M. *Anal. Biochem.* **1976**, *72*, 248−254.

(29) Kim, Y.; Ho, S. O.; Gassman, N. R.; Korlann, Y.; Landorf, E. V.; Collart, F. R.; Weiss, S. *Bioconjugate Chem.* **2008**, *19*, 786−791.

(30) Humphrey, W.; Dalke, A.; Schulten, K. *J. Mol. Graphics* **1996**, *14*, 27−38.

(31) St-Jean, M.; Sygusch, J. *J. Biol. Chem.* **2007**, *282*, 31028−31037.

(32) (a) Kuzmic, P. *Methods Enzymol.* **2009**, *467*, 247−280. (b) Kuzmic, P. *Anal. Biochem.* **1996**, *237*, 260−273.

(33) Agarwal, P. K.; Billeter, S. R.; Rajagopalan, P. T.; Benkovic, S. J.; Hammes-Schiffer, S. *Proc. Natl. Acad. Sci. U. S. A.* **2002**, *99*, 2794−2799.

(34) Pezza, J. A. Interactions among Isozyme-Specific Residues in Fructose-1,6-bisphosphate Aldolase. Ph.D. Thesis, Boston University, 2006.

(35) Wilkinson, A. J.; Fersht, A. R.; Blow, D. M.; Winter, G. *Biochemistry* **1983**, *22*, 3581−3586.

(36) Dalby, A.; Dauter, Z.; Littlechild, J. A. *Protein Sci.* **1999**, *8*, 291−297.

(37) Rose, I. A.; O'Connell, E. L. *J. Biol. Chem.* **1977**, *252*, 479−482.

(38) (a) Kellinger, M. W.; Johnson, K. A. *Biochemistry* **2011**, *50*, 5008−5015. (b) Kellinger, M. W.; Johnson, K. A. *Proc. Natl. Acad. Sci. U. S. A.* **2010**, *107*, 7734−7739.

(39) Kirmizialtin, S.; Nguyen, V.; Johnson, K. A.; Elber, R. *Structure* **2012**, *20*, 618−627.

(40) Guth, E. C.; Francklyn, C. S. *Mol. Cell* **2007**, *25*, 531−542.

(41) Gromadski, K. B.; Rodnina, M. V. *Mol. Cell* **2004**, *13*, 191−200.




DOI: 10.1021/jacs.5b08149
*J. Am. Chem. Soc.* 2015, 137, 13876−13886